Selection of a Remote Phosphor Configuration to Enhance the Color Quality of White LEDs

Nguyen Doan Quoc Anh[1]*, Phan Xuan Le[2], and Hsiao-Yi Lee[3]*

[1]*Power System Optimization Research Group, Faculty of Electrical and Electronics Engineering,
Ton Duc Thang University, Ho Chi Minh City, Vietnam*
[2]*Faculty of Electrical and Electronics Engineering, HCMC University of Food Industry,
Ho Chi Minh city, Vietnam*
[3]*Department of Electrical Engineering, National Kaohsiung University of Sciences and Technology,
Kaohsiung, Taiwan*

The remote phosphor structure has been proven to bear greater luminous efficiency than both the conformal phosphor and in-cup phosphor structures; however, controlling its color quality is much more challenging. To solve this dilemma, various researchers have proposed dual-layer phosphor and triple-layer phosphor configuration as techniques to enhance the display brightness of white LEDs (WLEDs). Likewise, this study picked one of these configurations to utilize in multichip WLEDs with five distinct color temperatures in the range from 5600 to 8500 K, for the purpose of improving the optical properties of WLEDs, such as color rendering index (CRI), color quality scale (CQS), luminous efficacy (LE), and chromatic homogeneity. According to the results of this research, the triple-layer phosphor configuration has superior performance compared to other configurations in terms of CRI, CQS, and LE, and yields higher chromatic stability for WLEDs.

I. INTRODUCTION

Phosphor-converted WLEDs have been predicted to widely displace conventional incandescent and fluorescent lamps in the lighting industry in the future, due to their high potential for considerable energy savings, great efficacy, compactness, low cost, and chromatic stability [1-4]. WLEDs, which work on the principle of combining blue light from a blue chip with yellow light from a phosphor [5-8], bear two profoundly beneficial characteristics that set them apart from conventional light sources such as incandescent and fluorescent lamps, which are (i) the capability to yield light with huge efficiency and (ii) that the properties of the light, such as spectral composition, can be controlled at a level that is infeasible for other light sources [9-12]. In generic phosphor-converted white light diode (pc-WLED) configurations, the most common method to create white light is via freely dispersed coating, in which the transparent encapsulated resin is combined with yellow-emitting phosphor powders and then dispersed in a cup reflector, or directly coated on the LED chip's surface. This approach can allow the thickness of the phosphor layer to be controlled efficiently, and hence greatly reduce the cost, but does not produce high-quality WLEDs, due to the energy losses and thermal effect caused by the LED chip [13]. On the contrary, the conformal-coating phosphor structure is more favorable for distributing colors uniformly, reducing the angular deviation of correlated

*Corresponding author: nguyendoanquocanh@tdtu.edu.vn, ORCID 0000-0001-7477-4701
leehy@nkust.edu.tw, ORCID 0000-0002-6296-461X

Color versions of one or more of the figures in this paper are available online.

color temperature (CCT), although its backscattering effect may decrease the luminous efficiency of WLEDs [14].

Previous studies have introduced the approach to separate the chip and the phosphor layer, in remote phosphor structures [15, 16]. Using a polymer hemispherical shell lens with an interior phosphor coating help enhance light extraction inside the reflection structure [17]. Furthermore, an air-gap embedded structure can also enhance luminous efficiency by reflecting light so that it heads down instead [18].

It is crucial for WLEDs to have good optical properties, including color rendering index (CRI), color quality scale (CQS), luminous efficacy (LE), and color uniformity. There have been reports on multilayer structures in remote phosphor configurations [15-20]; among them, the two advanced remote phosphor structures used to improve the aforementioned features are the dual- and triple-layer phosphor configurations. In the dual-layer phosphor configuration, the yellow phosphor layer is beneath a red or green phosphor layer, while the triple-layer phosphor configuration has three different phosphor layers: the yellow phosphor layer below, the red phosphor layer above, and the blue phosphor in the middle. Beside the package structure, the concentration of phosphor plays a vital role in luminous efficiency. Specifically, if the phosphor concentration increases, the loss of re-absorption in the phosphor layer also rises, causing a drop in the device's luminous efficiency, especially devices with lower CCTs [21]. To eliminate this phenomenon, it is essential to enhance the emission of blue and yellow rays and reduce the amount of light lost to backscattering and reflection.

In the face of many different methods, as mentioned above, it is tough for manufacturers to consider finding a suitable remote phosphor structure to mass fabricate their LEDs products with desirable efficiency. Therefore, this study proposes a novel technique for improving the optical properties of WLEDs. In addition, information on the applications, potentials, and challenges of WLEDs in the lighting industry is also discussed.

II. PREPARATION AND SIMULATION

2.1. Preparation of Phosphor Materials

The two ideas behind this study to enhance the luminous efficacy of LEDs are (i) utilizing the green phosphor layer $SrBaSiO_4:Eu^{2+}$ to enrich the green light component in WLEDs, leading to an increase in luminous flux, and (ii) improving the red light component in WLEDs, to advance CRI and CQS by employing the red phosphor layer $Sr_wF_xB_yO_z:Eu^{2+},Sm^{2+}$. This article also includes in detail the degree to which the chemical composition of $Sr_wF_xB_yO_z:Eu^{2+}$, Sm^{2+} affects the optical properties of WLEDs.

As can be seen, $SrBaSiO_4:Eu^{2+}$ and $Sr_wF_xB_yO_z:Eu^{2+},Sm^{2+}$ particles have been known as a type of yellow-green phosphor and have become increasingly popular, due to their various outstanding properties such as great quantum efficiency and stability at high temperature [22]. Thereby, they are particularly applied for extreme high-loading and long-lifetime fluorescent lamps.

The chemical compositions of $SrBaSiO_4:Eu^{2+}$ and $Sr_wF_xB_yO_z:Eu^{2+},Sm^{2+}$ are respectively presented in Tables 1 and 2, and need to be analyzed in detail before being applied to WLEDs, due to a sharp influence on each phosphor's optical properties. Specifically, $SrBaSiO_4:Eu^{2+}$

TABLE 1. Composition of yellow-green-emitting $SrBaSiO_4:Eu^{2+}$ phosphor

Ingredient	Mole (%)	By weight (g)	Molar mass (g/mol)	Mole (mol)	Ions	Mole (mol)	Mole (%)
$SrCO_3$	31.28	145	147.63	0.982	Sr^{2+}	0.982	0.088
$BaCO_3$	31.79	197	197.34	0.998	Ba^{2+}	0.998	0.090
SiO_2	33.40	63	60.08	1.049	Si^{4+}	1.049	0.094
Eu_2O_3	0.32	3.5	351.926	0.01	O^{2-}	8.068	0.726
NH_4Cl	3.22	5.4	53.49	0.101	Eu^{2+}	0.02	0.002

TABLE 2. Composition of red-emitting $Sr_wF_xB_yO_z:Eu^{2+},Sm^{2+}$ phosphor

Ingredient	Mole (%)	By weight (g)	Molar mass (g/mol)	Mole (mol)	Ions	Mole (mol)	Mole (%)
$Sr(NO_3)_2$	10.09	126.98	211.63	0.6	Sr^{2+}	0.6	0.0241
SrF_2	5.43	40.58	125.62	0.32	F^-	0.646	0.0259
H_3BO_3	84.12	309.2	61.83	5	B^{3+}	5	0.203
Eu_2O_3	0.25	5.28	351.93	0.015	O^{2-}	18.665	0.748
Sm_2O_3	0.11	2.09	348.72	0.006	Eu^{2+}	0.03	0.0012
$Sr_wF_xB_yO_z:Eu^{2+},Sm^{2+}$					Sm^{2+}	0.012	0.00048

emits yellow-green light at a peak wavelength of 525 nm, while $Sr_wF_xB_yO_z:Eu^{2+},Sm^{2+}$ emits red light at wider peak wavelengths over a range: 684, 693, 697, 703, 723, 725, and 732 nm. The presence of the Sm^{2+} ion helps to excite absorption at the peaks at 395, 420, and 502 nm. The condition for these phosphors to be applied is to have a consistent spectrum with blue light from the LED chip, which means the absorption spectra of these phosphors must match the spectrum of the blue chip. The absorption spectrum of $Sr_wF_xB_yO_z:Eu^{2+},Sm^{2+}$ ranges from 250 nm to 502 nm, which is favorable for absorbing light emitted from different bands, as there is not only blue light emitted but also yellow light, converted from the yellow phosphor layer. Similarly, $SrBaSiO_4:Eu^{2+}$ also has a wide absorption spectrum, ranging from 350 nm to 480 nm with an absorption efficiency of over 70%.

Before the optical simulation of the $SrBaSiO4:Eu^{2+}$ and $Sr_wF_xB_yO_z:Eu^{2+},Sm^{2+}$ particles is carried out, the input parameters—including phosphor concentration, phosphor particle size, excitation spectrum, absorption spectrum, and phosphor emission spectrum—need to be accurately determined by experiment. According to the results of a preceding studies [21], the luminous flux and angular chromatic homogeneity are involved with particle size, depending on the applied phosphor concentration and desired color temperature. Specifically, enlarging the particle size is advantageous for enhancing luminous flux, but yields inferior angular color stability. Hence, among the five parameters above, the phosphor concentration and particle size have to be defined to achieve the highest color quality and luminescent flux of WLEDs, whereas the spectral parameters are constants. However, as demonstrated in previous researches [21], the ideal diameter of the phosphor particles was suggested to be stabilized at an average of 14.5 μm.

2.2. Simulation Process

As illustrated in Fig. 1(a), this study uses WLEDs with nine LED chips inside, which have been constructed identically. The normalized cross correlations of the actual packaging and the simulated packaging are almost the same. Moreover, the impacts of LED wavelength, waveform, light intensity, and operating temperature on the CRI and CCT can be decreased. The LightTools program is utilized to simulate the phosphor compounding of WLEDs, in which the YAG:Ce^{3+} weight is controlled. The output of each blue chip is 1.16 W at the peak wavelength of 453 nm. The details of LED configuration specifications are provided in Fig. 1(b), including information on the lead frame, LED chip, die attachment, gold wire, and phosphor. Figure 1(c) presents a single-layer remote phosphor structure (Y) with a yellow phosphor layer YAG:Ce^{3+} on the surface of the LEDs. Figure 1(d) shows a dual-layer remote phosphor structure (YG) with a red phosphor layer $Sr_wF_xB_yO_z:Eu^{2+}$, Sm^{2+} above a yellow phosphor layer YAG:Ce^{3+}. As can be seen from Fig. 1(e), another dual-layer remote phosphor

Lead frame: 4.7 mm Jentech Size-S

LED chip: V45H

Die attach: Sumitomo 1295SA

Gold Wire: 1.0 mil

Phosphor: ITC NYAG4_EL

(a)   (b)

(c)   (d)
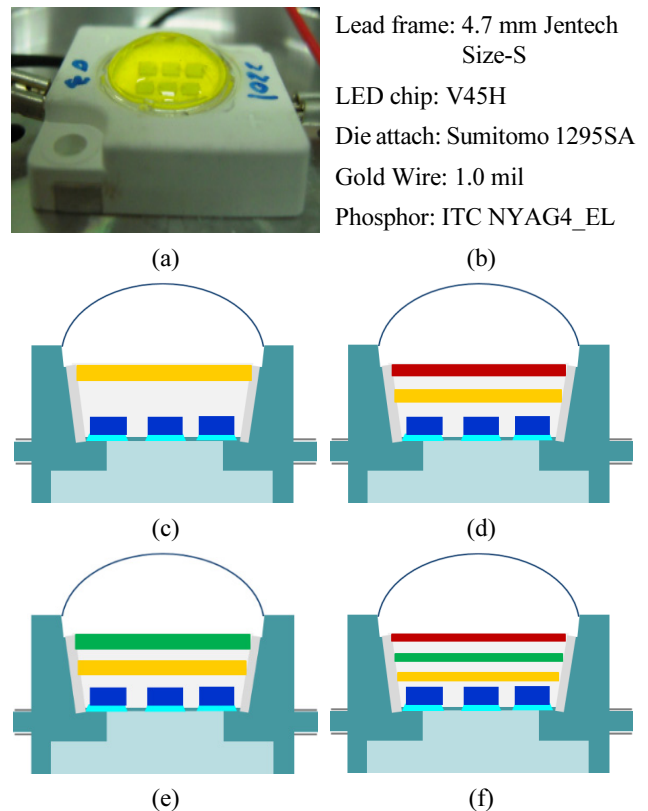

(e)   (f)

FIG. 1. Illustration of multilayer phosphor structures of white LEDs: (a) The actual MCW-LEDs and (b) its parameters, and the (c) single-layer phosphor dual-layer remote phosphor with (D) YR and (e) YG, and (f) triple-layer phosphor (YRG).

structure (YG) includes a green phosphor layer $SrBaSiO_4:Eu^{2+}$ above a yellow phosphor layer YAG:Ce^{3+}. Finally, the triple-layer remote phosphor structure (YRG) has a green phosphor layer $SrBaSiO_4:Eu^{2+}$ between a yellow phosphor layer YAG:Ce^{3+} and a red phosphor layer $Sr_wF_xB_yO_z:Eu^{2+}$, Sm^{2+}, as depicted in Fig. 1(f).

The thickness of these remote phosphor layers is 0.08 mm. To maintain the average correlated color temperature (ACCT), the concentration of YAG:Ce^{3+} needs to be varied according to the concentration of yellow phosphor or red phosphor. At each different ACCT for each phosphor structure, the YAG:Ce^{3+} concentration is also different. This distinguishes the scattering characteristic of the LEDs to create the differences in optical properties.

It can be seen in Fig. 2 that the weight percent of yellow-emitting YAG:Ce^{3+} phosphor is always highest in the Y structure and lowest in the YRG structure, regardless of ACCT. Considering the same ACCT in the remote phosphor structures, the higher the YAG:Ce^{3+} concentration, the higher the backscattering potential, causing a reduction in luminous flux. Conversely, there will be an imbalance of the three colors that produce the white light (green, red, and yellow) if the YAG:Ce^{3+} concentration is high, leading to a decrease in the color quality of the WLED. Therefore, to improve the luminous flux and brightness of WLEDs, it
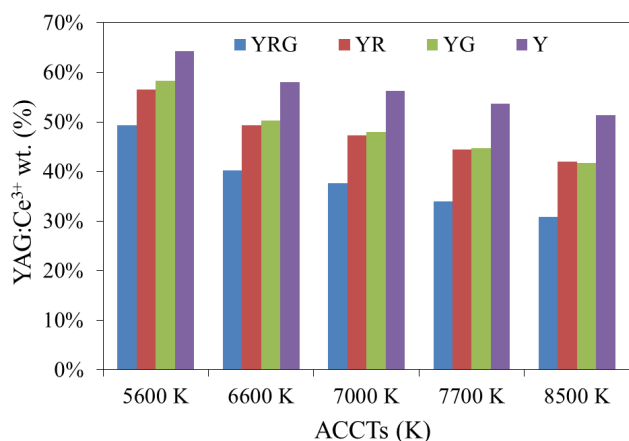
FIG. 2. Yellow-emitting YAG:Ce^{3+} phosphor concentration corresponding to each remote phosphor structure, at each of the different ACCTs.

is desirable to reduce backscattering and maintain the stability of these three basic colors. In addition, the color rendering index can be controlled by increasing the red light component. Besides, adjusting the green light component can control the chromatic homogeneity and luminescence. The triple-layer phosphor structure is considered to be the most advantageous in controlling the optical properties of WLEDs. However, relevant information regarding remote phosphor structures as well as the emission spectrum is about to be given following.

Obviously there is a distinct discrepancy in the emission spectrum of the different remote phosphor structures. The Y emitter spectrum has the lowest intensity, compared to the other three remote phosphor structures at five ACCTs. This confirms that the luminous flux yielded by the Y structure is the smallest. In contrast, the YRG structure produces the highest spectral intensity in the wavelength range of 380~780 nm, as shown in Fig. 3. In another
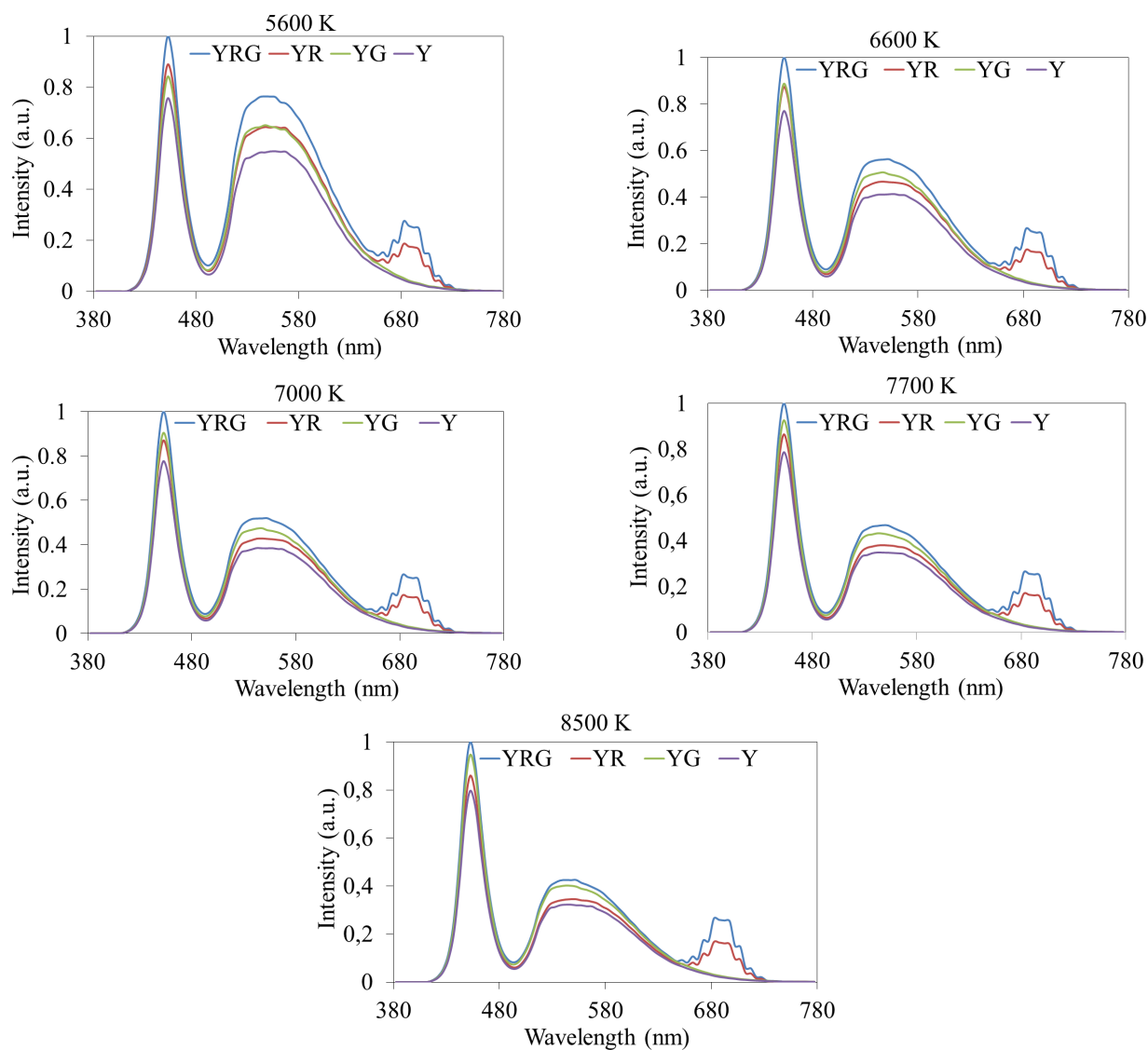

FIG. 3. Emission spectra of phosphor configurations for five ACCTs.

wavelength range of 400~500 nm, the YG structure's spectral intensity is greater than that of the YR structure, and therefore YG's luminous flux may be higher than YR's. However, the spectral intensity of YR is higher than that of YG in the range of 650~750 nm, which gives YR a better color rendering index than YG. All of the information mentioned above will be verified in Section III.

III. RESULTS AND DISCUSSION

Figure 4 illustrates the comparison of CRI values among the four remote phosphor structures Y, YR, YG, and YRG. It is obvious that the higher the ACCT, the higher the CRI, and the peak CRI value is achieved at ACCT of 8500 K. Controlling CRI is a challenge for remote phosphor structures, especially for structures with high ACCTs (greater than 7000 K), except for the YR structure, because this structure always achieves the highest CRI regardless of the ACCT, which is an essential foundation for advancing the CRI of these remote phosphor structures. In terms of the CRI value, the YR structure is most favorable for yielding high CRI, due to the red light component added from the red phosphor layer $Sr_wF_xB_yO_z:Eu^{2+},Sm^{2+}$. Meanwhile, the YRG structure dominates the second, and the YG structure ranks last, because it produced the lowest CRI value. Therefore, if the goal is to design WLEDs with higher CRI values, YR structures can be selected for mass production.

Nevertheless, CRI is just one of the indicators of color quality. In recent years the color quality scale (CQS), a combination of CRI, visual preference, and color coordinates, has become a research target of many studies, and seems to be the most vital optical indicator for evaluating color quality. In this paper the CQS of different phosphor configurations corresponding to ACCTs is compared in Fig. 5. While the YR reached the highest CRI, the YRG produced the highest CQS, which is the result of balance in the three basic colors (yellow, red, and green). On the other hand, the Y structure provides the lowest CQS, and hence its color quality is challenging to control, without the addition of red and green light components. This structure, though, has advantages in luminous flux and low cost, because its fabrication procedure is much simpler than for other structures.

From the results of Fig. 5, it can be concluded that if the manufacturer's objective emphasizes color quality, then the YRG structure is an appropriate option. However, a comparison of luminous flux emitted from the single-layer and dual-layer phosphors needs to be conducted, to determine whether the luminescence is affected during the improvement of color quality.

Next, a mathematical model of the transmitted blue light and converted yellow light in a multilayer phosphor structure, which provides a huge improvement in LED efficiency, will be presented and demonstrated. The
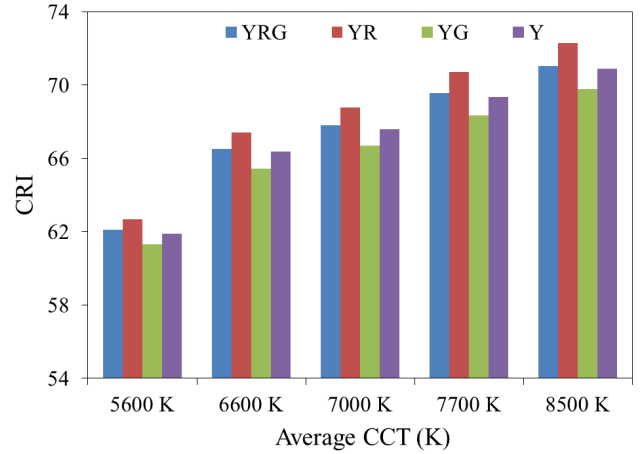

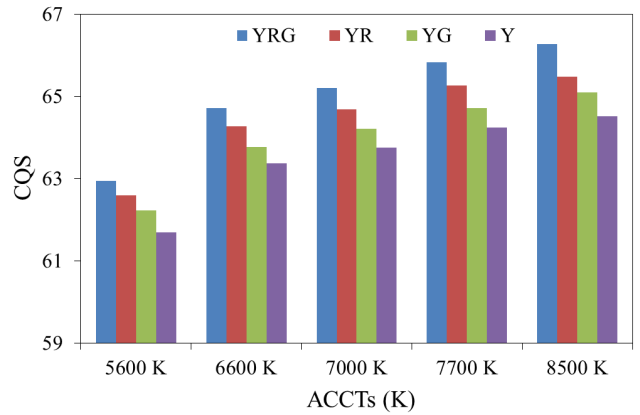FIG. 4. Color rendering indices of phosphor configurations for five ACCTs.

FIG. 5. Color quality scale of phosphor configurations for five ACCTs.

transmitted blue light and converted yellow light for a single-layer remote phosphor package with phosphor layer thickness of $2h$ are expressed as follows [23]:

$$PB_1 = PB_0 \times e^{-2\alpha_{B1}h} \tag{1}$$

$$PY_1 = \frac{1}{2} \frac{\beta_1 \times PB_0}{\alpha_{B1} - \alpha_{Y1}} (e^{-2\alpha_{Y1}h} - e^{-2\alpha_{B1}h}) \tag{2}$$

where the intensities of blue light (PB) and yellow light (PY) are the light intensity from the blue LED, indicated by PB_0. α_B and α_Y are parameters describing the fraction of energy lost for blue and yellow light respectively during propagation in the phosphor layer.

The transmitted blue light and converted yellow light for a dual-layer remote phosphor package with phosphor layer thickness of h are defined as:

$$PB_2 = PB_0 \times e^{-2\alpha_{B2}h} \tag{3}$$

$$PY_2 = \frac{1}{2}\frac{\beta_2 \times PB_0}{\alpha_{B2} - \alpha_{Y2}}(e^{-2\alpha_{Y2}h} - e^{-2\alpha_{B2}h}) \tag{4}$$

The subscripts "1" and "2" are used to describe the single- and dual-layer remote phosphor packages respectively. β is the conversion coefficient for blue light being converted to yellow light. γ is the reflection coefficient of the yellow light.

The lighting efficiency of WLEDs with the dual-layer phosphor structure is enhanced considerably, compared to one with the single-layer structure:

$$\frac{(PB_2 + PY_2) - (PB_1 + PY_1)}{PB_1 + PY_1} > 0 \tag{5}$$

The scattering of phosphor particles was analyzed using Mie theory and the Lambert-Beer Law [24]. The power of the transmitted light can be calculated by:

$$I = I_0 \ exp(-\mu_{ext}L) \tag{6}$$

In this formula, I_0 is the incident light power, L is the phosphor layer thickness (in mm) and μ_{ext} is the extinction coefficient, which can be expressed as $\mu_{ext} = N_r.C_{ext}$, where N_r is the number-density distribution of particles (in mm^{-3}) and C_{ext} (in mm^2) is the extinction cross section of phosphor particles.

Eq. (6) demonstrates that using multiple layers of phosphor is more advantageous for luminous flux than using just a single layer. This result can be verified in Fig. 6, in which the Y structure with a single phosphor layer achieves the lowest luminous flux among the four structures, at all ACCTs. This is definitely converse to the YRG structure, which obtains the highest luminous flux, due to its three phosphor layers. Thanks to the green phosphor SrBaSiO$_4$:Eu^{2+}, the YG structure yields the second-highest luminous flux after the YRG structure. The green phosphor layer helps to increase the green light and the spectrum in the range of 500~600 nm. Apparently in
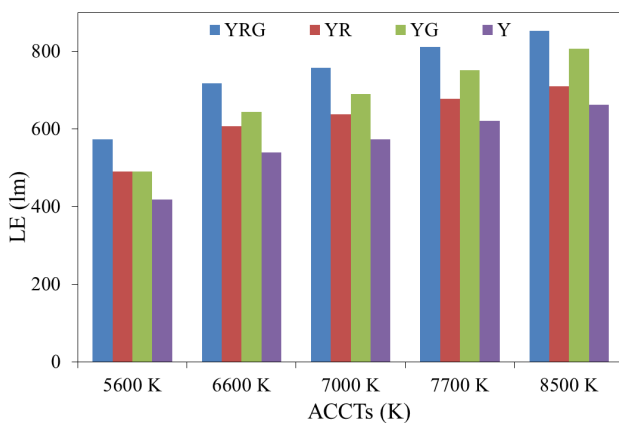
this wavelength range the intensity of YRG is greater than that of YG and Y, due to the smallest phosphor YAG:Ce^{3+} concentration in the YRG structure, to maintain the ACCT. Simultaneously, the YRG structure decreased the light scattering after YAG:Ce^{3+} concentration dropped. The blue rays from the LED chip easily transmit through YAG:Ce^{3+} to other layers. In other words, the YRG structure makes the blue-light energy conversion from the LED chip efficient. As a result, the YRG's spectral intensity is highest, compared to other remote phosphor structures in the white-light wavelength range. Accordingly, the luminous flux yielded by the YRG structure is also the highest.

As a result, the YRG structure can be selected, due to its outstanding optical properties, including CQS and LE. However, color uniformity cannot be neglected when it comes to color quality. There are a number of methods for improving chromatic stability, including the use of advanced scattering materials such as SiO$_2$ or CaCO$_3$, or employing a conformal phosphor configuration. Although color uniformity can be well improved, luminous efficiency can be significantly reduced if two methods are utilized. The use of green phosphor SrBaSiO$_4$:Eu^{2+} and red phosphor Sr$_w$F$_x$B$_y$O$_z$:Eu^{2+},Sm^{2+} not only increases the scattering properties, but also adds green or red light inside WLEDs, to produce better white light. The use of the remote phosphor structure enhances the luminous flux emitted, due to the drop in reflection back to the LED chip. However, it is essential to control the concentration of the phosphor layer appropriately to achieve the highest transmission power. This can be proved by the Lambert-Beer law in Eq. (6).

To evaluate the color uniformity of WLEDs, we determine how much variation there is among CCT values at different angles. This is an important standard for evaluating the performance of solid-state lighting applications. A large deviation in CCT with respect to angle will cause the "yellow ring" phenomenon and generate nonuniform white color at different angles. The angular CCT deviation [25, 26] is calculated as

$$\text{D-CCT} = \text{CCT}_{(Max)} - \text{CCT}_{(Min)} \tag{7}$$

where $\text{CCT}_{(Max)}$ and $\text{CCT}_{(Min)}$ represent the maximal CCT (occurring at a viewing angle of zero degrees) and minimal CCT (occurring at 90 degrees) respectively.

Figure 7 shows the comparison of correlated color temperature deviation (D-CCT) for four remote phosphor configurations, at five different ACCTs. Obviously YRG has the smallest color deviation, and hence its color homogeneity will be the highest, which is the result of the scattering inside the LED package before the formation of white light. Besides, structures with more phosphor layers will yield more scattering events, which helps to increase the color uniformity of WLEDs, but may lead to a drop in brightness. However, this decline is negligible, compared to the benefit of reducing backscattering. Thus the YRG structure can efficiently produce chromatic homogeneity

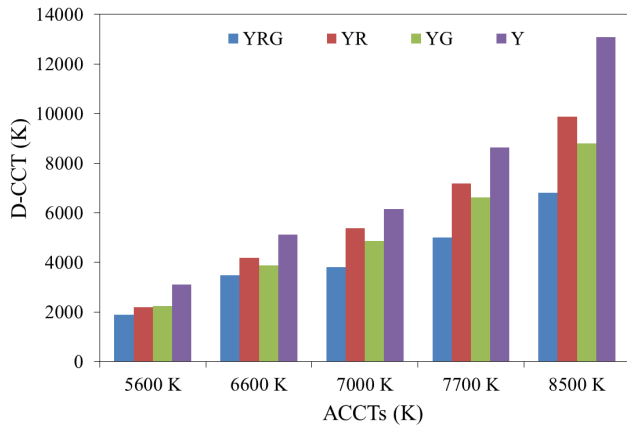FIG. 6. Luminous efficacy of phosphor configurations for five ACCTs.

FIG. 7. Correlated color temperature deviation (D-CCT) of remote phosphor configurations for five ACCTs.

without affecting the luminous flux, while the color deviation was highest for the Y structure at all ACCTs.

IV. CONCLUSION

To conclude, a comparison of luminescence efficacy among four structures (Y, YG, YR, and YRG) at five ACCTs was presented in this article, where the simulation process featured the green phosphor SrBaSiO$_4$:Eu^{2+} and red phosphor Sr$_w$F$_x$B$_y$O$_z$:Eu^{2+},Sm^{2+}, while the results were verified using Mie theory and the Lambert-Beer Law. Accordingly, the coating of the yellow-green-emitting phosphor SrBaSiO$_4$:Eu^{2+} to complement the green light aims to enhance color uniformity and luminous flux, and consequently the YG structure achieves better optical and color uniformity than the YR structure. CRI and CQS can be improved by increasing the red light component through the red phosphor layer Sr$_w$F$_x$B$_y$O$_z$:Eu^{2+},Sm^{2+}. As a result, the YR structure achieves higher CRI and CQS than does YG. However, the problem is that the color quality depends tightly on the balance of the three colors (yellow, green, and red), and it is the YRG structure that can satisfy this three-color control requirement. In addition, the degradation of the YRG layer's backscattering helps to increase the luminous flux of this configuration. The evidence shows that the highest achievable luminous efficacy is also yielded by the YRG structure. The results of this paper ease manufacturers in picking a proper phosphor configuration to advance the performance of WLEDs.

ACKNOWLEDGEMENT

REFERENCES

1. P. T. Tin, N. K. H. Nguyen, M. Q. H. Tran, and H.-Y. Lee, "Red-emitting α-SrO·3B$_2$O$_3$:Sm^{2+} phosphor for WLED lamps: novel lighting properties with two-layer remote phosphor package," Curr. Opt. Photon. **1**, 389-395 (2017).
2. Q. Zhang, R.-L. Zheng, J.-Y. Ding, and W. Wei, "Excellent luminous efficiency and high thermal stability of glass-in-LuAG ceramic for laser-diode-pumped green-emitting phosphor," Opt. Lett. **43**, 3566-3569 (2018).
3. M.-M. Jiao, C.-L. Yang, M.-L. Liu, Q.-F. Xu, Y. J. Yu, and H.-P. You, "Mo^{6+} substitution induced band structure regulation and efficient near-UV-excited red emission in NaLaMg(W,Mo)O$_6$:Eu phosphor," Opt. Mater. Express **7**, 2660-2671 (2017).
4. R. Liu, L.-J. Liu, and Y.-J. Liang, "Energy transfer and color-tunable luminescence properties of YVO$_4$:RE (RE = Eu^{3+}, Sm^{3+}, Dy^{3+}, Tm^{3+}) phosphors via molten salt synthesis," Opt. Mater. Express **8**, 1686-1694 (2018).
5. T. Hayashida, H. Iwasaki, K. Masaoka, M. Shimizu, T. Yamashita, and W. Iwai, "Appropriate indices for color rendition and their recommended values for UHDTV production using white LED lighting," Opt. Express **25**, 15010-15027 (2017).
6. P.-Q. Jiang, Y. Peng, Y. Mou, H. Cheng, M. X. Chen, and S. Liu, "Thermally stable multi-color phosphor-in-glass bonded on flip-chip UV-LEDs for chromaticity-tunable WLEDs," Appl. Opt. **56**, 7921-7926 (2017).
7. S. Kim, F. Iqbal, and H.-S. Kim, "Relationship between phosphor properties and chromaticity of phosphor-in-glass," Appl. Opt. **56**, 9477-9483 (2017).
8. H. Daicho, K. Enomoto, H. Sawa, S. Matsuishi, and H. Hosono, "Improved color uniformity in white light-emitting diodes using newly developed phosphors," Opt. Express **26**, 24784-24791 (2018).
9. H. F. Sijbom, R. Verstraete, J. J. Joos, D. Poelman, and P. F. Smet, "K$_2$SiF$_6$:Mn^{4+} as a red phosphor for displays and warm-white LEDs: a review of properties and perspectives," Opt. Mater. Express **7**, 3332-3365 (2017).
10. Y. Peng, X. Guo, R.-X. Li, H. Cheng, and M.-X. Chen, "Thermally stable WLEDs with excellent luminous properties by screen-printing a patterned phosphor glass layer on a microstructured glass plate," Appl. Opt. **56**, 3270-3276 (2017).
11. J.-F. Ruan, Z.-W. Yang, H.-L. Zhang, J.-B. Qiu, Z.-G. Song, and D.-C. Zhou, "Phase transformation induced reversible modulation of upconversion luminescence of WO$_3$:Yb^{3+}, Er^{3+} phosphor for switching devices," Opt. Lett. **43**, 3885-3888 (2018).
12. L. Wang, X.-J. Wang, K. Takahashi, T. Takeda, N. Hirosaki, and R.-J. Xie, "Nitride phosphors as robust emissive materials in white flat field emission lamps," Opt. Mater. Express **7**, 1934-1941 (2017).
13. Y. Peng, Y. Mou, X. Guo, X.-J. Xu, H. Li, M. X. Chen, and X.-B. Luo, "Flexible fabrication of a patterned red phosphor layer on a YAG:Ce^{3+} phosphor-in-glass for high-power WLEDs," Opt. Mater. Express **8**, 605-614 (2018).
14. B.-Y. Joo and J.-H. Ko, "Analysis of color uniformity of white LED lens packages for direct-lit LCD backlight applications," J. Opt. Soc. Korea **17**, 506-512 (2013).

15. Z.-T. Li, H.-Y. Wang, B.-H. Yu, X.-R. Ding, and Y. Tang, "High-efficiency LED COB device combined diced V-shaped pattern and remote phosphor," Chin. Opt. Lett. **15**, 042301 (2017).

16. S.-W. Jeon, S.-H. Kim, J. Choi, I. Jang, Y.-H. Song, W.-H. Kim, and J. P. Kim, "Optical design of dental light using a remote phosphor light-emitting diode package for improving illumination uniformity," Appl. Opt. **57**, 5998-6003 (2018).

17. X.-R. Ding, Q. Chen, Y. Tang, J.-S. Li, D.-P. Talwar, B.-H. Yu, and Z.-T. Li, "Improving the optical performance of multi-chip LEDs by using patterned phosphor configurations," Opt. Express **26**, A283-A292 (2018).

18. S.-D. Yu, Y. Tang, Z.-T. Li, K.-H. Chen, X.-R. Ding, and B.-H. Yu, "Enhanced optical and thermal performance of white light-emitting diodes with horizontally layered quantum dots phosphor nanocomposites," Photon. Res. **6**, 90-98 (2018).

19. X.-Y. Huang, S.-Y. Wang, B. Li, Q. Sun, and H. Guo, "High-brightness and high-color purity red-emitting $Ca_3Lu(AlO)_3(BO_3)_4$:Eu^{3+} phosphors with internal quantum efficiency close to unity for near-ultraviolet-based white-light-emitting diodes," Opt. Lett. **43**, 1307-1310 (2018).

20. T.-H. Yang, S.-M. Wu, C.-C. Sun, B. Glorieux, C.-Y. Chen, Y.-Y. Chang, X.-H. Lee, Y.-W. Yu, T.-Y. Chung, and K.-Y. Lai, "Stabilizing CCT in pcW-LEDs by self-compensation between excitation efficiency and conversion efficiency of phosphors," Opt. Express **25**, 29287-29295 (2017).

21. S. Liu, and X. B. Luo, *LED Packaging for Lighting Applications: Design, Manufacturing and Testing* (Chemical Industry Press and John Wiley & Sons, Beijing, 2011).

22. W. M. Yen and M. J. Weber, *Inorganic Phosphors: Compositions, Preparation and Optical Properties* (CRC Press, LLC, 2000 N.W. Corporate Blvd., Boca Raton, Florida 33431, 2004).

23. B. Li, D. Zhang, Y. Huang, Z. Ni, and S. Zhuang, "A new structure of multi-layer phosphor package of white LED with high efficiency," Chin. Opt. Lett. **8**, 221-223 (2009).

24. Z.-Y. Liu, S. Liu, K. Wang, and X.-B. Luo, "Measurement and numerical studies of optical properties of YAG:Ce phosphor for white light-emitting diode packaging," Appl. Opt. **49**, 247-57 (2010).

25. N. D. Q. Anh, M. F. Lai, H. Y. Ma, and H. Y. Lee, "Enhancing of correlated color temperature uniformity for multi-chip white-light LEDs by adding SiO_2 to phosphor layer," J. Chin. Inst. Eng. **38**, 297-303 (2015).

26. N. D. Q. Anh and H. Y. Lee, "Improving the angular color uniformity and the lumen output for white LED lamps by green $Ce_{0.67}$ $Tb_{0.33}$ $MgAl_{11}$ O_{19}:Ce,Tb phosphor," J. Chin. Inst. Eng. **39**, 871-875 (2016).